Rotational and Translational Motions of Trapped Methane. Incoherent Inelastic Neutron Scattering of Methane Hydrate†

John S. Tse* and Christopher I. Ratcliffe

Steacie Institute for Molecular Sciences, National Research Council of Canada, Ottawa, Ontario, Canada K1A 0R6

Brian M. Powell and Varley F. Sears

AECL Research, Chalk River Laboratories, Chalk River, Ontario, Canada K0J 1J0

Y. Paul Handa

Institute for Environmental Chemistry, National Research Council of Canada, Ottawa, Ontario, Canada K1A 0R6

Received: September 30, 1996; In Final Form: December 13, 1996⊗

The temperature dependence of the rotational and translational motion of methane encaged in a deuterated clathrate hydrate has been studied with incoherent inelastic neutron scattering. The methane molecules were found to behave almost like free rotors even at 6 K. The most interesting observation is that, unlike methane deposited in rare-gas matrices, the rotational modes do not converge to the classical rotation−diffusion limit at high temperature. The spectral features indicate that the methane interacts strongly with the host lattice vibrations and its motion is damped at high temperature. The methane vibrational density of states obtained from the experiment using a self-consistent iterative procedure to correct for multiexcitation and multiple scattering effect is found to be in good agreement with molecular dynamics calculations.

1. Introduction

Clathrate hydrates are nonstoichiometric inclusion compounds with the host framework composed of water molecules stabilized through the inclusion of a variety of guest atoms and molecules in the cavities.[1] An individual cavity is large enough to encage only a single guest.[2,3] This unique structural feature makes clathrate hydrates suitable matrices for molecular isolation.[4] The presence of the guests also gives the clathrate hydrates some very unusual thermophysical properties when compared to ice. For instance, the memory effect in pressure-amorphized hydrates,[5] the very large thermal expansivity,[6] and the glasslike thermal conductivity[7] can be attributed to the unique guest−host interactions.

The anomalous thermal conductivity is perhaps the single most intriguing property of clathrate hydrates.[7−11] Despite the well-defined crystalline structures,[2,3] the temperature dependence of the thermal conductivity deviates from that found in normal crystals and resembles that of an amorphous material.[7] Moreover, the profile and magnitude of the thermal conductivity show little influence of either the host structure or the nature of the guest.[10,11] The basic mechanisms responsible for this very interesting phenomenon are not fully understood. Molecular dynamics calculations show that the guest vibrations are localized modes.[12−15] Analysis of the experimental thermal conductivity data of tetrahydrofuran hydrate[7] suggests further that resonant interactions[16,17] between these localized guest vibrations and the heat-carrying host acoustic phonons may greatly enhance the phonon-scattering processes and thus may be responsible for the glassy thermal behavior. The exact nature of the resonant scattering is, however, undefined due to insufficient experimental information. Two possible mechanisms can be offered to explain the strong coupling of the host and guest vibrations.[18] The localized guest vibrations may interact and exchange energy with the continuum elastic host lattice waves through an Anderson−Fano[19,20] type process or via avoided-crossing of the acoustic branches of the phonon dispersion curves. In principle, these proposals can be examined by measuring the phonon dispersion curves of a clathrate hydrate from coherent inelastic neutron scattering. This experiment, however, requires a fairly large single crystal. Since most simple clathrate hydrates are stable only under pressure or at very low temperature,[1] the synthesis of large single crystals is a nontrivial problem, and this may be the reason that, to date, no such experiment has been performed.

Methane hydrate is an important prototype for clathrate hydrates. The recent discovery of natural gas hydrates[22,23] rich in methane has stimulated extensive study of their electrical, physical, and thermochemical properties. The rotational motion of methane has long been a subject of intense interest,[24,25] and the interpretation of the results will benefit from comparison with other inelastic neutron scattering studies. Moreover, results from theoretical molecular dynamics calculations are available for comparison.[14] This paper reports results of a study of the dynamical properties of methane (CH_4) in a polycrystalline deuterated (D_2O) structure I clathrate hydrate sample using inelastic incoherent neutron scattering (IINS). The objectives of this investigation are to examine the low-frequency localized modes associated with the rotational and translational motions of the guest and to study the nature of the guest−host interactions.

II. Experimental Section

Sample Preparation. Deuterated structure I methane hydrate (ideal stoichiometry $CH_4 \cdot 5.75D_2O$) was prepared as described previously.[26] Research grade CH_4 (from Matheson) with minimum purity of 99.95 mol % was mixed in the appropriate

† Publish as NRCC 40824.

⊗ Abstract published in *Advance ACS Abstracts,* May 15, 1997.

S1089-5639(96)03006-X CCC: $14.00 Published 1997 by the American Chemical Society

amount with powdered deuterated ice in a Parr pressure vessel loaded with stainless steel rods. The vessel was placed on a set of rollers and rotated about its long axis at −20 °C. The tumbling motion of the steel rods provided the grinding action required to speed up the reaction between ice and gas. The reaction was completed within 24 h, as indicated by the steady pressure reading. The vessel was then kept overnight in dry ice, and the sample was then recovered by cooling to liquid nitrogen temperature in the absence of the excess pressure. The purity of the hydrate samples was checked by X-ray diffraction and calormetric measurements. For the IINS experiment, about 1 g of the hydrate was spread evenly and tightly packed between two sheets of thin aluminum, which were then clamped together in the sample holder. The thickness of the sample is 2 mm, and the sample area exposed to the neutron beam is about 80 cm^2. Finally, the holder was attached to the cold tip of a liquid-helium cryostat. The entire handling process was conducted under liquid nitrogen to avoid water condensation or hydrate decomposition. The integrity of the sample was verified from its powder neutron diffraction pattern.

Inelastic Incoherent Neutron Scattering. Inelastic incoherent neutron scattering experiments were made on the C5 spectrometer at the NRU reactor, Chalk River. Several hydrate samples were used from different batches to demonstrate reproducibility. Measurements over a wide (*ca.* 3 THz) frequency range were made with Si[111] reflections as both monochromator and analyzer. A fixed analyzing energy of 2.5 THz was used, and the energy resolution (fwhm) was 0.14 THz. The wave vector transfer, Q, was 2.14 $Å^{-1}$, and data were taken at temperatures of 5, 20, and 77 K. Measurements at higher resolution over a more restricted (*ca.* 0.6 THz) frequency range were made with a Si[111] monochromator and a graphite [0002] analyzer. With a fixed analyzing energy of 1.2 THz the energy resolution (fwhm) was 0.045 THz. A cold Be filter was placed in the scattered beam to eliminate higher order neutrons. The wave vector transfer for these measurements was 1.87 $Å^{-1}$, and data were collected at 5.3, 10, and than at 5 K intervals up to 30 K.

Data Treatment and Analysis. The scattering function $S(Q,\omega)$ that characterizes the incoherent scattering of thermal neutrons in condensed matter is, in the Gaussian approximimation,[27] determined by the velocity spectrum $Z(\omega)$, which is the Fourier transform of the velocity autocorrelation function of the scattering atom. For a harmonic crystal the Gaussian approximation is in fact exact, and if the crystal is also cubic with one atom per unit cell (e.g. a bcc or fcc structure), $Z(\omega)$ is equal to the phonon density of states. Otherwise, $Z(\omega)$ not only depends on the phonon frequencies but is also weighted by the phonon polarization vectors. However, the velocity spectrum is defined for any system and the corresponding "multiphonon" expansion of $S(Q,\omega)$[28]—in which the 1-phonon term is proportional to $Z(\omega)$ and the contribution from n-phonon processes is given as a convolution of the 1-phonon and n-phonon terms—is valid as long as the atoms are localized in space so that the Debye−Waller factor is nonvanishing. In particular, it is valid for the present case of methane hydrate.

Since the incoherent scattering cross section of the proton is[29] very much larger than the cross sections of any of the other nuclides in the present system of CH_4 in D_2O clathrate, the neutron scattering by the system is due almost entirely to incoherent scattering by the H atoms in the methane molecules. The IINS measurements therefore allow one to determine the velocity spectrum $Z(\omega)$ of the H atoms and, hence, to obtain information about the translational and rotational motion of the methane molecules in their cages.

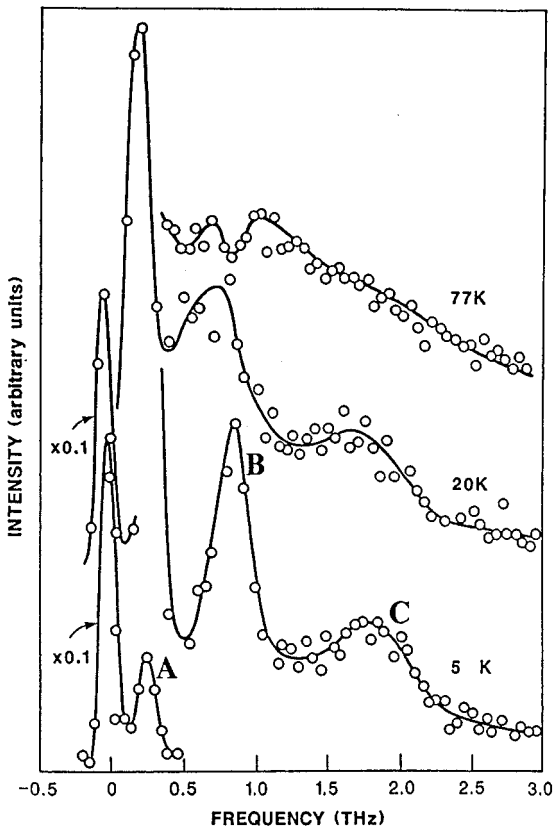

Figure 1. Inelastic incoherent neutron scattering spectra for deuterated methane hydrate at 5, 20, and 77 K (1 THz = 33.3 cm^{-1}).

In determining $Z(\omega)$, the correction for "multiphonon" scattering was made using a self-consistent, iterative method in which the measured inelastic scattering was taken as the zeroth-order approximation. This is a well-known method that has recently been applied in, for example, the determination of the phonon density of states of crystalline and amorphous ice.[30] To ensure that the truncation error was less than 0.1%, it was necessary to include up to 5-phonon processes, and self-consistency was achieved after three iterations.

Molecular Dynamics Calculations. Previous molecular dynamics (MD) calculations on methane hydrate[13,14] were performed at high temperatures on a small system. To complement the experimental work, MD calculations in the microcanonical (N,V,T) ensemble were repeated at a lower temperature using a structure I hydrate model consisting of 368 water and 64 methane molecules ($2 \times 2 \times 2$ unit cells). The intermolecular potential parameters and the technical details of the calculations are the same as those reported previously.[14] All the MD calculations were performed at 67.8 K. Attempts to equilibrate the system at lower temperature were successful due to mode-locking, and thermodynamic equilibration cannot be achieved. The H atom vibrational density of states $Z(\omega)$ was evaluated from the Fourier transform of the relevant single-particle velocity autocorrelation function.

III. Results

The uncorrected IINS spectra for CH_4 hydrate at 5, 20, and 77 K are shown in Figure 1. The features in the spectra are dominated by the CH_4 vibrations since the bound incoherent scattering length for the proton is much greater than for deuterium.[29] Three main energy loss peaks are readily identified from the low-temperature spectra. At 5 K, a sharp peak A is observed at 0.25 THz (8.3 cm^{-1}) as well as two broad bands B and C located at 0.83 THz (27.7 cm^{-1}) and 1.80 THz (60.0

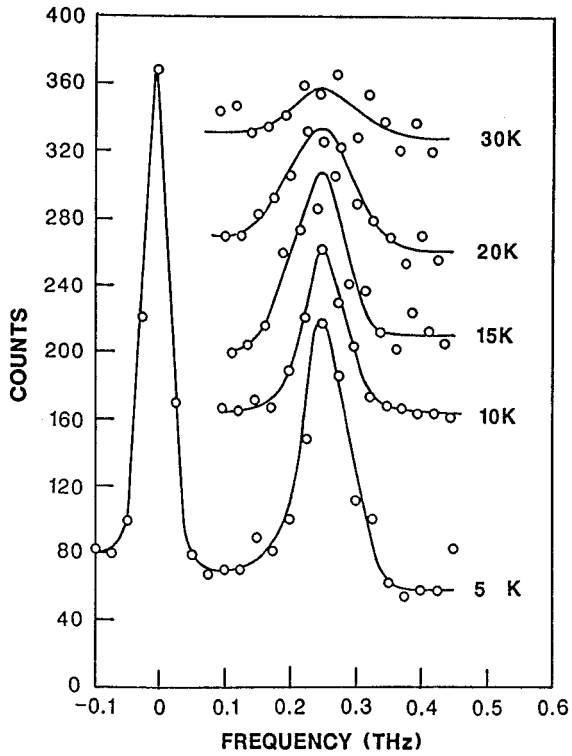

Figure 2. Temperature dependence of the CH_4 $J = 0 \rightarrow 1$ rotational excitation transition in deuterated methane hydrate.

cm^{-1}), respectively. As will be explained later, peak A can be assigned to the rotational motion and peaks B and C to the translation motions of the guest molecules. The spectral features show a very strong temperature dependence. The increase in line width with temperature is particularly pronounced for peak A. To investigate this behavior further, high-resolution IINS spectra in the low-energy region were measured as a function of temperature (Figure 2). It is significant to note that even though the line width increases substantially with temperature, the peak position remains unchanged. At 35 K, peak A becomes so broad it merges into the background. In contrast, the higher energy translational peaks B and C behave in a different manner. Their line shapes in Figure 1 broaden and shift slightly to lower energies when the temperature is raised. At 77 K, the highest temperature studied, peak C becomes a shoulder of a broad band, and it appears that peak B may have split into two peaks.

IV. Discussion

Rotational Motion. The frequency of the low-energy feature A is similar to that in the high-temperature phase of solid methane (II)[31] and CH_4 isolated in rare-gas matrices.[32] This peak is assigned to the $J = 0 \rightarrow 1$ quantum rotational excitation inside the clathrate hydrate cages. At 5 K, 95% of the CH_4 molecules are in their ground rotational state. The observed rotational transition energy of 8.3 cm^{-1} can be compared with those of CH_4 trapped in solid argon, krypton, and xenon matrices, which are 7.18, 7.90, and 9.10 cm^{-1}, respectively.[32] These values are close to the free rotor limit of 10.5 cm^{-1}, indicating that the rotational motion is only slightly perturbed by the molecular field created by the water molecules forming the cavity. As the depth of the potential increases the $0 \rightarrow 1$ transition frequency decreases. The almost hindered rotation of CH_4 in the clathrate hydrate is a direct confirmation of the weak van der Waals host−guest interactions. This observation correlates with the results from ^1H NMR T_1 relaxation time measurements, which show that the CH_4 execute rapid and effectively isotropic rotation even at 4 K.[33] The experimental finding is also in accord with the almost uniform orientational order parameters[34] evaluated from molecular dynamics calculations[14] which imply the CH_4 molecules are rotating freely about all inertial axes and show little preference for any specific orientation. It is noteworthy that despite the fact that methane occupies the two types of cages in structure I hydrates, there is no indication of inequivalent CH_4 molecules in the rotational spectrum.

Additional evidence for almost nonhindered rotating CH_4 molecules can be obtained from a study of the intensity variation of the inelastic scattering peak with the neutron wave vector momentum transfer Q. For a free rotor, the scattered intensities (I) are approximately proportional to the spherical Bessel function $j_1^2(Qr)$,[35−37]

$$I = Aj_1^2(Qr)$$

where A is a constant and r is the CH bond length. A comparison of the calculated fit to the experimental intensity is shown in Figure 4. The agreement is quite satisfactory in view of the simplicity of the theoretical model. An effective C−H bond distance of 1.23 ± 0.05 Å extracted from the least squares fit is reasonably close but not equivalent to the true isolated CH bond of 1.093 Å. The discrepancy may be attributed to a small rotational−translational coupling that was not accounted by the simple model.[38]

The thermal behavior of CH_4 rotational excitations in the clathrate hydrate is of particular significance. In matrix isolated CH_4,[32] the rotational excitation peak widens and shifts to lower energy and eventually merges with the central elastic scattering peak as the temperature is increased. The continuous transition from almost free quantum rotation at low temperatures to classical rotational diffusion at high temperatures is due to strong coupling of the rotation and translational motion in these systems. This trend, however, is observed in the clathrate hydrate. The line width, intensity, and position of the inelastic scattering peak A and the intensity of the central elastic scattering peak are shown in Figure 3. It is remarkable that while the frequency and total intensity of peak A remain fairly constant, the line width increases when the temperature is raised from 5 to 35 K. There is no indication of deterioration in instrument resolution, as the intensity of the elastic peak shows no significant variation.

The different behavior of the temperature dependence of the rotational peak may be attributed to restricted motion of the CH_4 due to enclathration. A similar behavior in the rotational line shape has been reported for 4-methylpyridine[39,40] and molecular hydrogen coordinated to transition metals.[41] In both cases, the methyl group and the hydrogen molecule have a remarkable freedom of rotation, but the translational motions are strongly hindered by the bonding interactions. The temperature dependence of the rotational peak observed previously and also here is consistent with the prediction from a phenomenological model[42] which suggests that the broadening and shift in the inelastic scattering line shape is due to the coupling of the rotator to the low-frequency acoustic phonons in the host lattice. The low-frequency phonon spectrum for ice shows a distribution of acoustic modes maximized at 70 cm^{-1}.[43] It is expected that the density of vibrational states of clathrates will be similar to that in ice.[12,14,44] Therefore, it is reasonable to expect that the CH_4 motion will couple with the acoustic phonons, although the exact mechanism of this coupling is still unknown. A detailed understanding of this process would be extremely important in the understanding of the effects of weak intermolecular interactions on the dynamics of this system.

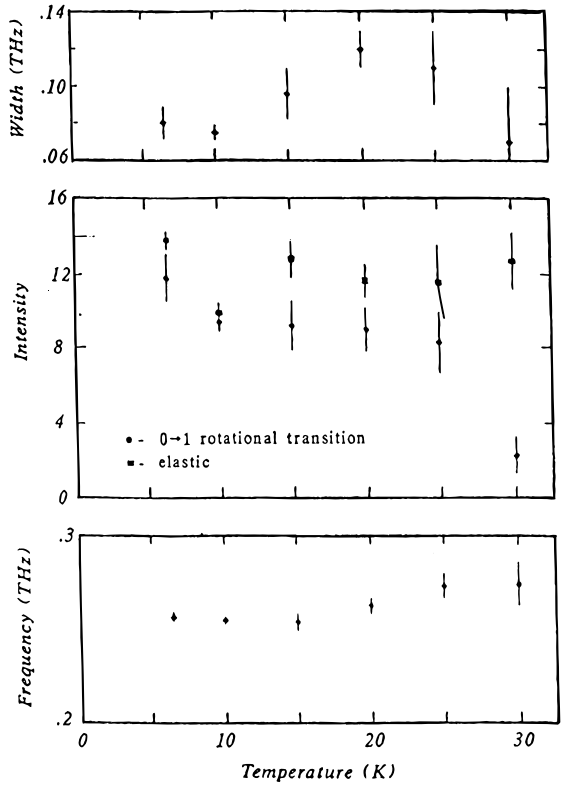

Figure 3. Temperature dependence of the CH_4 $J = 0 \rightarrow 1$ rotational excitation line shape: line width (top); total integrated intensity (middle); and energy loss (bottom).

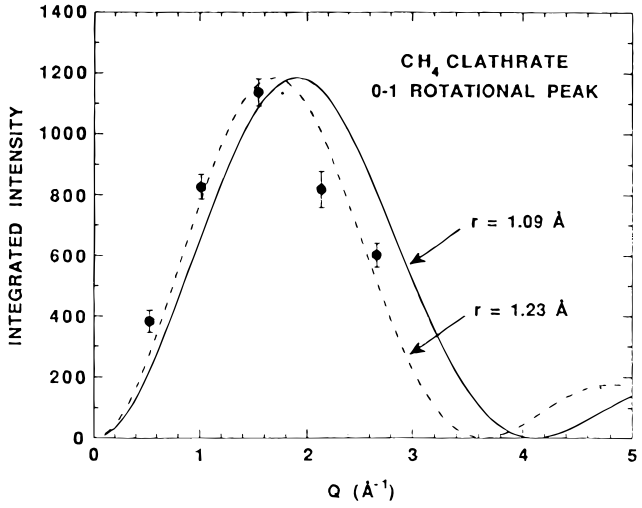

Figure 4. Integrated intensity of the rotation excitation peak as a function of neutron wave vector Q. The solid curve is calculated from the approximation model (see text) using $r = 1.09$ Å, and the dashed curve is the result of a least squares fit to the data, which gives an effective CH bond of 1.23 ± 0.05 Å.

In the studies of CH_4 deposited in rare-gas matrices[32] much weaker lines were observed which were assigned to higher order rotational transitions. However, the two other main peaks observed at 27.7 and 60 cm^{-1} in the IINS spectrum of CH_4 hydrate do not follow the same pattern of frequency increases. Unfortunately, the rotational potential in CH_4 hydrate is unknown, and so it is not possible to calculate expected frequencies for the higher transitions, but there is strong evidence to suggest that these two peaks are, in this case, primarily due to the translational motions. In a very low hindered potential barrier, such as the one-dimensional methyl group rotor in 4-methylpyridine, the high-order transitions were not observed in the IINS spectrum.[36]

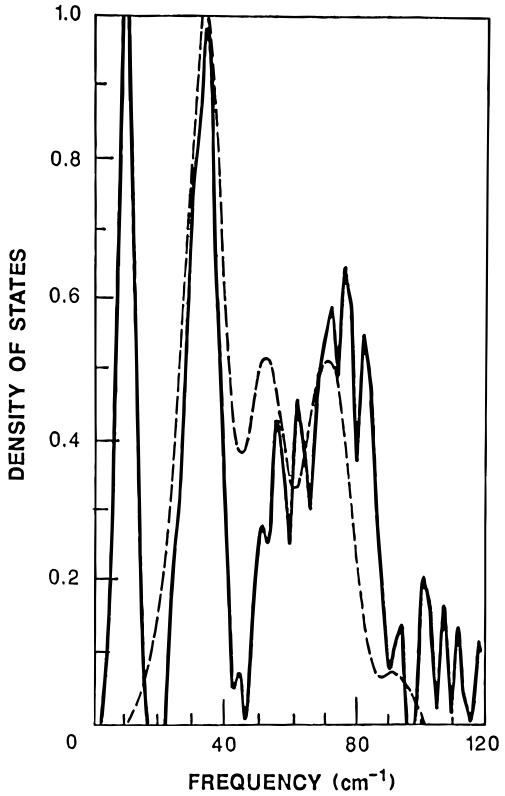

Figure 5. Experimental velocity spectrum $Z(\omega)$ (solid) and theoretical translational density of states (dashed) for CH_4 in deuterated methane hydrate.

Translational Motion. The translational modes of CH_4 in the hydrate cages are primarily localized rattling motions.[14] There is strong evidence supporting the assignment of the higher energy peaks B and C in Figure 1 to these motions. The translational vibrations of CH_4 enclathrated in β-hydroquinone[45] and deposited in a krypton matrix[46] are found to occur in the same energy region. The observed peak positions are also in reasonable agreement with the vibrational frequencies (47, 75 cm^{-1}) derived from an analysis of the guest contribution to the heat capacity of CH_4 hydrate employing the ideal solid−solution model.[47] Molecular dynamics calculations performed at 67.8 K predicted three phonon bands in the center-of-mass vibrational density of states: The highest energy peak at 69 cm^{-1} is due to the motions of CH_4 in the small and symmetric cavities, wheras the two calculated lower frequency vibrations at 27 and 48 cm^{-1} arise from CH_4 in the large cavities.[2] The splitting of approximately 20 cm^{-1} is due to the axial asymmetry of the large cages.[2] Hence, peaks B and C can be correlated with the local modes in the large and small cages, respectively. In view of the simplicity of the intermolecular potentials used, it is not surprising that the splitting is not reproduced accurately by the molecular dynamics calculations. A comparison of the calculated translational vibration density of states with the velocity spectrum $Z(\omega)$ derived from the IINS spectrum at 5 K is shown in Figure 5. Apart from the absence of the rotational line, which is not considered in the theoretical calculations, the calculated density of states is in qualitative agreement with the experimental $Z(\omega)$. Furthermore, the observation that the line width of peak C is almost twice that of peak A strongly suggests that the predicted second band, due to librations in the large cages, may contribute to peak C.

The line shapes of both translational bands broaden with increasing temperature. At high temperatures, the frequent collisions of CH_4 with the water molecules forming the cages shorten the lifetimes of the translational excitations. As

TABLE 1: Factor Group Analysis of the Translational Vibrations in the Small (G^S) and Large (G^L) Cavities of a Structure I Clathrate Hydrate[a]

cage	site symmetry	point group	vibrational symmetry
small, $[5^{12}]$	$m\bar{3}$	T_h	$T_{1u} + T_{2u}$
large, $[5^{12}6^2]$	$\bar{4}m2$	D_{2d}	$A_{2g} + E_g + T_{1g} + 2T_{1u} + T_{2u} + T_{2g}$

[a] Structure I hydrate: $G^S{}_2{\cdot}G^L{}_6{\cdot}46H_2O$. Space group: $Pm3n$ (no. 223) $O_h{}^3$. $\Gamma_{guest} = 3(T_{1u}) + 2T_{2u} + T_{1g} + T_{2g} + A_{2g} + E_g$. $\Gamma_{acoustic} = T_{1u}$.

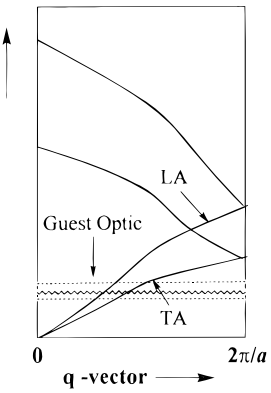

Figure 6. Schematic phonon dispersion curve illustrating the symmetry avoided-crossing between the lattice acoustic modes with the localized guest vibrations.

expected, this effect is more pronounced for CH_4 in the small cages than in the large cages. At 77 K, peak C is almost entirely under the slope of the broad band (Figure 1). It is interesting to observe that peak B is apparently split into two peaks separated by 10 cm^{-1}. However, this may be an artifact, but the relatively poor statistics at this temperature make it difficult to confirm this interpretation, and more precise measurements are needed.

V. Conclusion

It is shown here from the analysis of the IINS spectra that the CH_4 molecules enclathrated in the hydrate rotate almost freely, but the translational motions are localized. These observations and the experimental translational density of states are in reasonable agreement with the molecular dynamics calculations. The temperature dependence of the rotational line differs from CH_4 doped in rare-gas matrices and indicates possible coupling with the acoustic phonons of the water framework. Although the mechanism of this coupling is still yet to be determined, it may provide a means for the exchange of energy between the guest and the host and thus be responsible for the anomalous glassy behavior in the thermal conductivity. This suggestion is quite possible considering the symmetries of the lattice and the guest vibrations. A factor group analysis of the lattice acoustic and guest translational motions is summarized in Table 1. For the cubic space group the acoustic vibrations at the zone center transform as T_{1u} symmetry. The lattice acoustic modes are strongly dispersive and the longitudinal acoustic vibration reaches an energy maximum at about 140 cm^{-1}.[12,13] The guest vibrations in both the large and small cavities also possess T_{1u} symmetry. As the guest (CH_4) vibrations are found experimentally to be localized within 30−70 cm^{-1} and since the energy dispersions are small, there must be a symmetry avoided-crossing along certain phonon wave vectors between the zone center and the zone boundary. A schematic representation of this interaction is shown in Figure 6. The avoided-crossing of the guest and lattice phonon branches will promote energy transfer between them and affects the phonon scattering processes responsible for thermal conduction.

References and Notes

(1) Davidson, D. W. In *Water−A Comprehensive Treatise*; Frank, F., Ed.; Plenum Press: New York, 1973.
(2) McMullan, R. K.; Jeffrey, G. A. *J. Chem. Phys.* **1965**, *42*, 2725.
(3) Mak, T. C. W.; McMullan R. K. *J. Chem. Phys.* **1965**, *42*, 2732.
(4) Davidson, D. W.; Ripmesster, J. A. In *Inclusion Compounds*; Atwood, J. L., Davis, J. E. D., MacNicol, D. D., Eds.; Academic Press: New York, 1984; Vol. 3.
(5) Handa, Y. P.; Tse, J. S.; Klug, D. D.; Whalley, E. *J. Chem. Phys.* **1991**, *94*, 623.
(6) Tse, J. S.; McKinnon, W. R.; Marchi, M. *J. Phys. Chem.* **1987**, *91*, 4188.
(7) Tse, J. S.; White, M. A. *J. Phys. Chem.* **1988**, *92*, 5008.
(8) Stoll, R. D.; Bryan, G. M. *J. Geophys. Res.* **1979**, *B84*, 1629.
(9) Ross, R. P.; Andersson, P.; Backstrom, G. *Nature* **1981**, *290*, 322.
(10) Andersson, P.; Ross, R. G. *J. Phys.* **1983**, *C16*, 1423.
(11) Handa, Y. P.; Cook, J. G. *J. Phys. Chem.* **1981**, *91*, 1327, and references therein.
(12) Tse, J. S.; Klein, M. L.; McDonald, I. R. *J. Chem. Phys.* **1983**, *78*, 2096.
(13) Tse, J. S.; Klein, M. L.; McDonald, I. R. *J. Chem. Phys.* **1983**, *86*, 4198.
(14) Tse, J. S.; Klein, M. L.; McDonald, I. R. *J. Chem. Phys.* **1984**, *81*, 6146.
(15) Tse, J. S.; Klein, M. L. *J. Phys. Chem.* **1987**, *91*, 5789.
(16) Pohl, R. O. *Phys. Rev. Lett.* **1962**, *8*, 481.
(17) Seward, W. D.; Narayanamurti, V. *Phys. Rev.* **1966**, *148*, 463.
(18) Tse, J. S. *J. Incl. Related Phenom.* **1994**, *17*, 259.
(19) Anderson, P. W. *Phys. Rev.* **1961**, *124*, 41.
(20) Fano, U. *Phys. Rev.* **1961**, *124*, 1866.
(21) Walton, D.; Mook, H. A.; Nicklow, R. N. *Phys. Rev. Lett.* **1974**, *33*, 412.
(22) Cox, J. L. *Natural Gas Hydrates: Properties, Occurrence and Recovery*; Butterworth: London, 1983.
(23) Davidson, D. W.; Garg, S. K.; Gough, S. R.; Handa, Y. P.; Ratcliffe, C. I.; Ripmesster, J. A.; Tse, J. S. *Geochim. Cosmochim. Acta* **1986**, *50*, 619.
(24) Press, W. *Single Particle Rotations in Molecular Crytals*; Springer-Verlag: New York, 1981.
(25) *Inert Gases*; Klein, M. L., Ed.; Spinger Series in Chem. Phys.; Springer-Verlag: New York, 1984; Vol. 34.
(26) Handa, Y. P. *J. Chem. Thermodyn.* **1986**, *18*, 915.
(27) Rahman, A. H.; Singwi, K. L.; Sjolander, A. *Phys. Rev.* **1962**, *126*, 986.
(28) Sears, V. F. *Phys. Rev.* **1973**, *A7*, 340.
(29) Sears, V. F. In *Methods of Experimental Physics*; Skold, K., Price, D. L., Eds.; 1986; Vol. 23A, p 521.
(30) Klug, D. D.; Whalley, E.; Svensson, E. C.; Root, J. H.; Sears, V. F. *Phys. Rev.* **1991**, *B44*, 841.
(31) Press, W.; Kollmar, A. *Solid State Commun.* **1975**, *17*, 405.
(32) Kataoka, Y.; Press, W.; Buchenau, U.; Spitzer, H. In *Neutron Inelastic Scattering*; Proc. Symp., Vol. I.; Vienna, 1978; p 311.
(33) Garg, S. K.; Gough, S. R.; Davidson, D. W. *J. Chem. Phys.* **1975**, *63*, 1646.
(34) Klein, M. L.; McDonald, I. R.; Ozaki, Y. *J. Chem. Phys.* **1984**, *79*, 5579.
(35) Sears, V. F. *Can. J. Phys.* **1967**, *45*, 237.
(36) Ozaki, Y.; Kataoka, Y.; Yamamoto, T. *J. Chem. Phys.* **1980**, *73*, 3442.
(37) Asmussen, B.; Gerlach, P.; Press, W.; Prager, M.; Blank, H. *J. Chem. Phys.* **1989**, *90*, 400.
(38) Havighorst, M.; Prager, M.; Coddens, G. *Chem. Phys. Lett.* **1996**, *259*, 1.
(39) Abed, K. J.; Clough, S.; Carlile, C. J.; Rosi, B.; Ward, R. C. *Chem. Phys. Lett.* **1987**, *141*, 215.
(40) Filaux, F.; Carlile, C. J.; Kearley, G. J. *Phys. Rev.* **1991**, *B44*, 12280.
(41) Van der Sluys, L. S.; Eckart, J.; Eisenstein, O.; Hall, J. H.; Huffman, J. C.; Jackson, S. A.; Koetzle, T. F.; Kubas, G. J.; Vergamini, P. J.; Caulton, K. G. *J. Am. Chem. Soc.* **1990**, *112*, 4831.
(42) Hewson, A. C. *J. Phys.* **1982**, *C15*, 3855.
(43) Prask, H. J.; Trevino, S. F.; Gault, J. D.; Logan, K. W. *J. Chem. Phys.* **1972**, *56*, 3217.
(44) Tse, J. S.; Klein, M. L.; McDonald, I. R. *J. Chem. Phys.* **1984**, *81*, 6124.
(45) Burgiel, J. C.; Meyer, H.; Richards, P. L. *J. Chem. Phys.* **1965**, *43*, 4291.
(46) Nanba, T.; Sagara, M.; Ikezawa, J. *J. Jpn. Phys. Soc.* **1980**, *48*, 428.
(47) Handa, Y. P.; Tse, J. S. *J. Phys. Chem.* **1986**, *90*, 5917.